Experiments on defect spreading in hexagonal foams

1997 J. Phys.: Condens. Matter 9 8921

(http://iopscience.iop.org/0953-8984/9/42/008)

J. Phys.: Condens. Matter **9** (1997) 8921–8935. Printed in the UK PII: S0953-8984(97)84252-X

Experiments on defect spreading in hexagonal foams

M Fátima Vaz and M A Fortes

Departamento de Engenharia de Materiais, Instituto Superior Técnico, Av. Rovisco Pais 1096, Lisboa, Portugal

Received 13 May 1997, in final form 27 June 1997

Abstract. Defects were introduced in a hexagonal liquid foam prepared by a novel technique and their coarsening was observed. Both isolated defect clusters, with and without dislocation character, and grain boundaries were produced. As the defects coarsen, a gradient of cell size develops along the direction of growth. Differences in the growth characteristics of isolated defects were found, depending on whether the average size of the cells in the defect clusters is larger (type I) or smaller (type II) than the size of the surrounding honeycomb cells. Clusters of type I show an approximately linear increase of diameter with time, while clusters of type II have an initial contraction. The evolution to the scaling regime of a honeycomb containing a distribution of type I clusters is discussed.

1. Introduction

Computer simulations of the spreading of an isolated defect cluster embedded in a perfect hexagonal foam indicate that the radius of (round) clusters and the number of cells (bubbles or grains) in the cluster increase linearly with time at long times [1–3]. Contradictory results were obtained in relation to the long-term distribution of n, the number of sides of cells in the cluster. Levitan [1] found a stationary distribution distinct from the one reached from an initially random foam. While this result was questioned by Weaire [4], other simulations [2, 3] indicate a non-stationary distribution of n, with a second moment, μ_2, increasing continuously in time.

The spreading of a grain boundary between two misoriented honeycombs does not seem to have been studied. The coarsening of a line defect boundary between two polydisperse hexagonal foams was simulated by Herdtle and Aref [5], but they did not give any quantitative results. From the behaviour of isolated defects, the width of a grain boundary defect and the number of cells in it should increase linearly with time, at long times.

In this paper we describe experiments on defect spreading in hexagonal foams, which we compare with the predictions of the simulations. It should be noted, however, that the duration of our experiments was limited by breakdown of the foam after a few days, while most computer simulations describe results at long times, when the defects reach a 'statistically significant' state.

A detailed study of the topology of isolated defect clusters in hexagonal networks classified isolated defects into three main types [6]. Defects with $\langle n \rangle_c \neq 6$, where $\langle n \rangle_c$ is the average n of the cluster cells, have disclination character and are not considered in the present paper, since we were unable to produce them. Defects with $\langle n \rangle_c = 6$ may have dislocation character (Burgers vector $B \neq 0$) or be neutral ($B = 0$). Dislocation defects

0953-8984/97/428921+15$19.50

are surrounded by a hexagonal network containing extra half-rows of hexagons. Neutral defects are surrounded by a perfect honeycomb.

A defect cluster with N_c cells is surrounded by a 6-belt which is defined as the *shortest* circuit of hexagons (i.e. cells with six neighbours or 6-cells) encircling the defect. All cells in and outside the 6-belt are 6-cells. The number N_6 of 6-cells in the 6-belt is a measure of the perimeter of the defect. The number N of 6-cells that can be fitted inside the defect hole of a neutral defect to reconstruct the perfect honeycomb is a measure of the topological area of the defect. For dislocation defects, the topological area can be measured by a size number, N, which, for the purpose of this paper, is identified with the largest number of hexagons that can be fit inside the 6-belt. Both N_6 and N can be used to indicate the size of a defect cluster.

For a round cluster of radius R in a honeycomb with cells of area A and edge length a, we have

$$\begin{aligned} \pi R^2 &= NA \\ 2\pi R &= N_6 P_L^{-1} \end{aligned} \tag{1}$$

with

$$A = \frac{3\sqrt{3}}{2}a^2. \tag{2}$$

P_L is the number of edges of honeycomb cells intersected per unit length of randomly oriented test lines, with

$$P_L = \frac{2}{\pi}L_S. \tag{3}$$

L_S is the length of edges in the honeycomb per unit area:

$$L_S = \frac{3a}{A} = \frac{2}{\sqrt{3}a}. \tag{4}$$

Equations (1) assume that the 6-belt has equal size when it is filled with the defect or with honeycomb 6-cells. The area of the cluster is then proportional to N.

2. Experimental technique

The foams used in the experiments are monolayer foams, consisting of a layer of bubbles sandwiched between the originally free surface of a surfactant solution and a parallel glass plate above it. The bubbles are formed by blowing air through a fine nozzle into the detergent solution. As they form and come to the free surface of the liquid, they bridge to a glass plate above the free level of the solution. This plate covers the vessel containing the liquid (figure 1). The bubbles form a monolayer foam, which approximates a two-dimensional foam as the height of the monolayer increases. The height of the bubbles is quite uniform, even if the bubbles have different sizes, and is determined by the width of the gap between the liquid and the plate.

Hexagonal foams are easily obtained in this way by generating bubbles with the same volume. In order to form as perfect a foam as possible, the bubbles were introduced inside a regular hexagonal frame placed at the liquid surface level. The bubbles used in the experiments had an area A (parallel to the plate) of the order of a few mm^2 and heights of a few mm. Larger heights produce thinner liquid films (more rapid inter-bubble gas diffusion) but it is more difficult to obtain perfect foams.

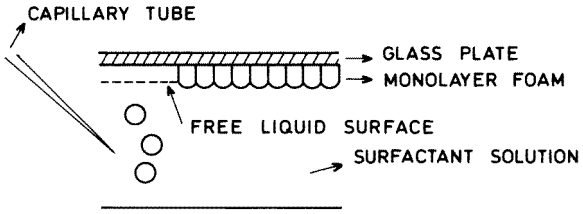

Figure 1. Schematic illustration of the technique used to prepare a monolayer hexagonal foam. The monolayer of bubbles is formed between the surface of a surfactant solution and a parallel plate above it.

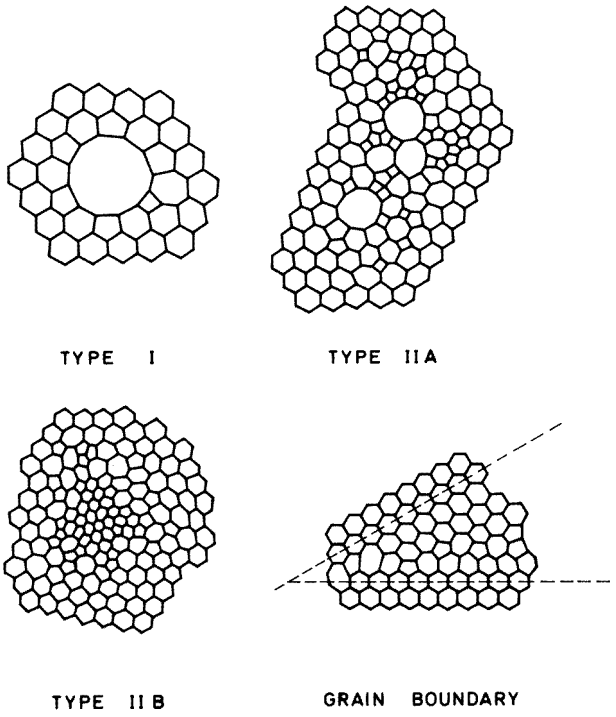

Figure 2. Schematic representation of the defects studied: defect clusters of types I, IIA and IIB, and grain boundary.

In a variant of this foam preparation technique [7], the plate is initially in contact with the liquid surface. The bubbles find room at the plate/liquid interface by pushing the liquid. This variant gives more perfect foams, but the height of the monolayer is determined by the volume of the bubbles and cannot be controlled independently.

The honeycomb foams produced by the monolayer technique are usually quite perfect but may contain a few pairs of adjacent cells with five and seven sides (5/7 pairs) which probably nucleate at the periphery of the foam as this is being formed. These defects do not interfere with the central defect during the lifetime of the experiments.

In the experiments done so far, the liquid fractions in the foams were relatively high; the bubbles are fairly round rather than polygonal. We will refer to such bubbles as 6-bubbles or 6-cells avoiding the term hexagonal.

The defect clusters were introduced in the hexagonal foam by blowing air bubbles with a syringe before the entire foam was formed. By controlling the flow rate of air from the syringe, defect clusters of various types were formed:

(i) type I clusters—clusters with one large central cell (area $A_m \gg A$) with many sides (m), surrounded by a layer or bilayer of cells with $n \neq 6$ (figure 2(a));

(ii) type IIA clusters—clusters which have several cells larger than the honeycomb cells, but they also contain small cells (figure 2(b)), so that the average area of a cell in the defect is smaller than the area, A, of the hexagonal surrounding cells;

(iii) type IIB clusters—clusters which contain exclusively small cells with area smaller than the area of the honeycomb cells (figure 2(c)).

While type I clusters initially have $N > N_c$, in type II clusters the reverse is true ($N < N_c$). Clusters with more than one large cell, for which $N > N_c$, can also be classified as being of type I, but will not be considered in the present paper.

Grain boundaries were formed by generating, side by side, two honeycombs differently oriented (figure 2(d)). A frame with a chosen angle was used in some cases.

3. Results

All defect clusters observed had $\langle n \rangle_c = 6$. Some had dislocation character, with extra half-rows of 6-cells in the surrounding hexagonal network. The Burgers vector $\bar{B}$ was determined by the method described in [6]. The defect of figure 4 has $\bar{B} = 0$ (neutral defect) while the defect of figure 3 has $\bar{B} = \bar{b}$ and that of figure 6 has $\bar{B} = 2\bar{b}$, where $\bar{b}$ is a vector between the centres of two adjacent 6-cells. The extra half-rows in a defect with dislocation character are indicated in figure 3.

For each defect cluster we have measured, as a function of ageing time, the following quantities:

N_c—number of cells in the cluster,

N_6—number of 6-belt cells,

N—size number of the cluster,

m—number of sides of larger cell in type I clusters,

μ_2, $(\mu_2)_6$—second moment of the distribution of the N_c cluster cells and of the $N_c + N_6$ cells, respectively,

D—the diameter of the cluster (average measurement in four different fixed directions).

Note that D is a poor measure of the linear dimension of a non-circular cluster.

For type I clusters we also obtained $(\mu_2)_w$, the second moment of the N_c cells in the defect excluding the large central cell with many sides.

For grain boundary defects we measured $\langle n \rangle_b$, the average number of sides of the cells in the defect (cells with number of sides different from six), the second moments μ_2, $(\mu_2)_6$ and an average width of the defect.

The area A of the 6-cells in the honeycombs was obtained from the measurement of the total area of a large number of cells.

3.1. Type I clusters

The evolution of two defects of this type is shown in figures 3 and 4. The defect of figure 3 has $\bar{B} = \bar{b}$ while that of figure 4 has $\bar{B} = 0$. The initial values of m of the large cell in the defects were 11 and 14, respectively for figure 3 and figure 4. Figure 5 shows, for a defect of

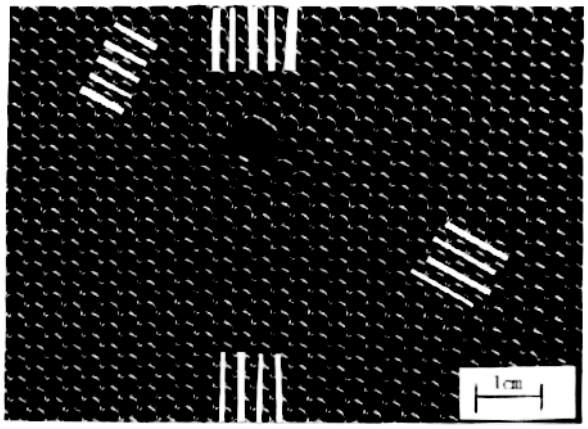

(a)

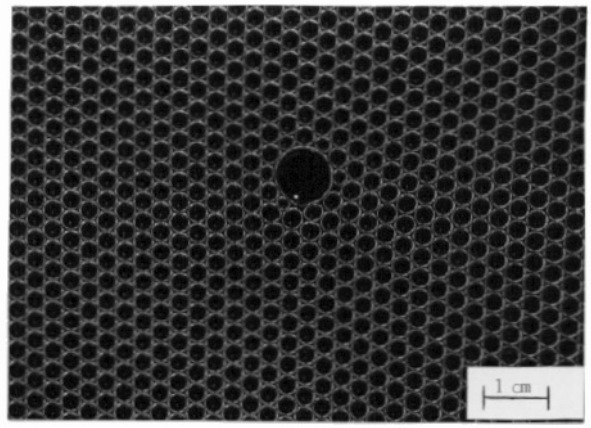

(b)

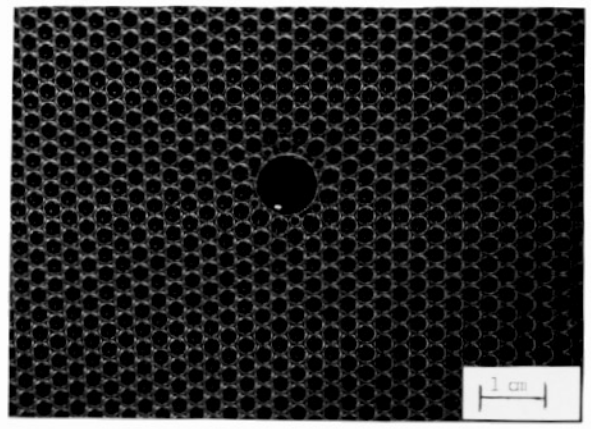

(c)

Figure 3. Evolution of a defect cluster of type I. (a) $t = 0$ h; (b) $t = 19$ h; (c) $t = 42$ h. The Burgers vector is $\bar{B} = \bar{b}$ and the associated extra half-rows are indicated by arrows.

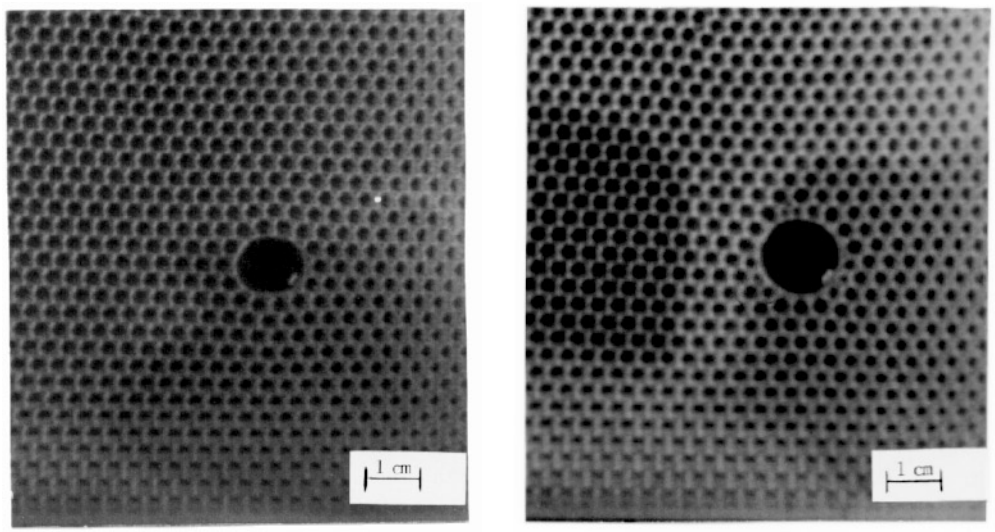

(a) (b)

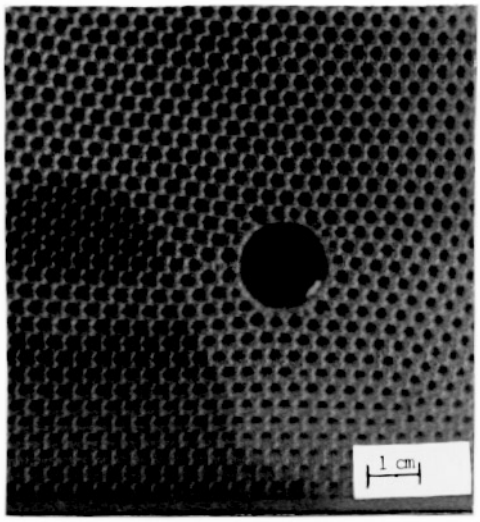

(c)

Figure 4. Evolution of a defect cluster of type I. (a) $t = 0$ h; (b) $t = 18$ h; (c) $t = 43$ h. The Burgers vector is $\vec{B} = 0$.

this type, the variation with time of the various quantities defined above: N_c, N_6, N, m, the second moments μ_2 and $(\mu_2)_6$ and the diameter D. The diameter was also calculated from N_6 and N using (1), showing good agreement with the measured values. Note that $N > N_c$ at all times. All quantities increase with time, although with fluctuations in some cases. The diameter, D, and the numbers N_6 and m increase approximately linearly. This agrees with the computer simulation results [1–3]. The defect cells around the larger central cell have a fairly invariant distribution with average n between 5.2 and 5.6 and $(\mu_2)_w$ between

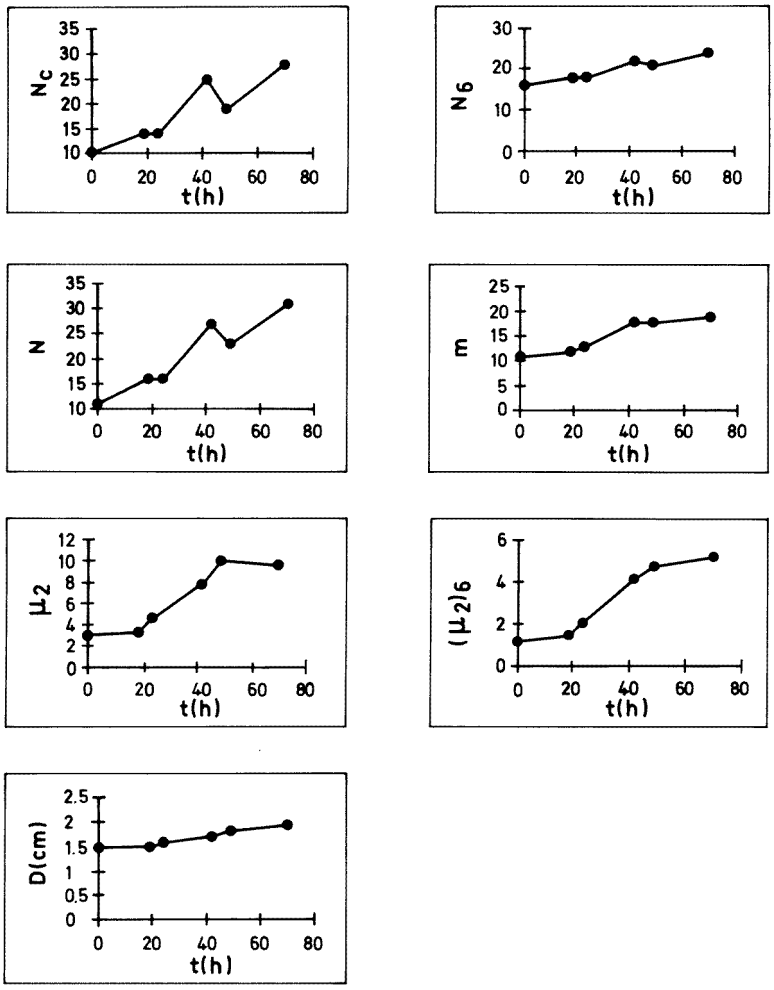

Figure 5. Evolution of various parameters of a type I defect cluster: N_c, N_6, N, m, μ_2, $(\mu_2)_6$ and diameter D.

0.5 and 1.5. This is in reasonable agreement with computer simulations [3] which indicate that a topologically invariant distribution of those cells is reached, with an average n around 5.5 and $(\mu_2)_w \approx 0.7$. The Burgers vector had no effect on the kinetics.

The measured variation of m with time has been used to estimate the kinetic constant k in von Neumann's law [8] for the rate change of the area A_n of a cell with n sides in a 2D foam:

$$\frac{\mathrm{d}A_n}{\mathrm{d}t} = k(n-6). \tag{5}$$

k is a characteristic property of the foam. The perimeter of the large bubble (area A_m) with m sides is $2(\pi A_m)^{1/2}$ and can be equated to $mP_L^{-1} = (\pi/2)mL_S^{-1}$ (see (3)); using (4) yields

$$m = \frac{8}{\sqrt{3\pi}} \frac{A_m^{1/2}}{a}. \tag{6}$$

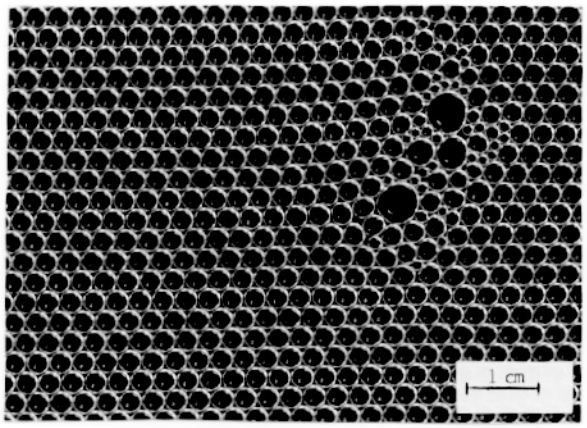

(a)

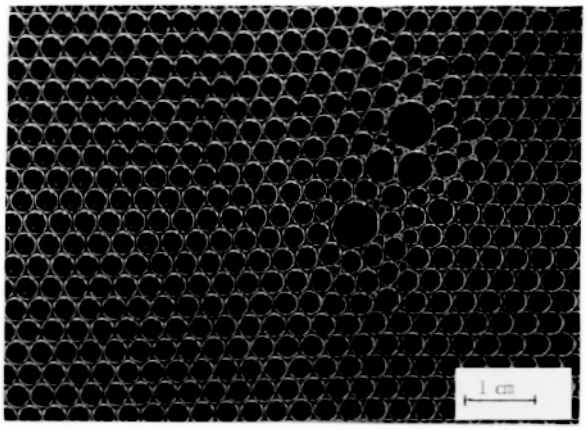

(b)

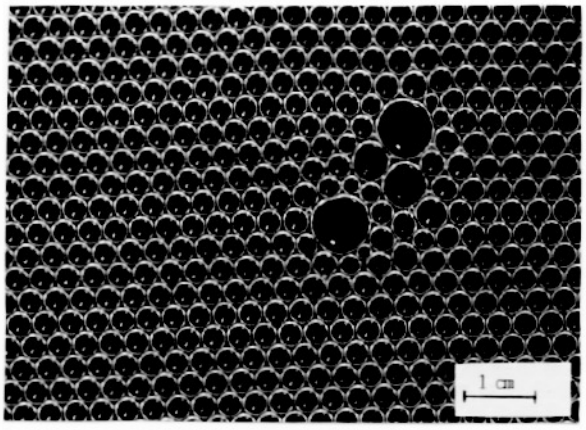

(c)

Figure 6. Evolution of a defect cluster of type IIA. (a) $t = 0$ h; (b) $t = 3$ h; (c) $t = 21$ h. The Burgers vector is $\bar{B} = 2\bar{b}$. There are two pairs of extra half-rows.

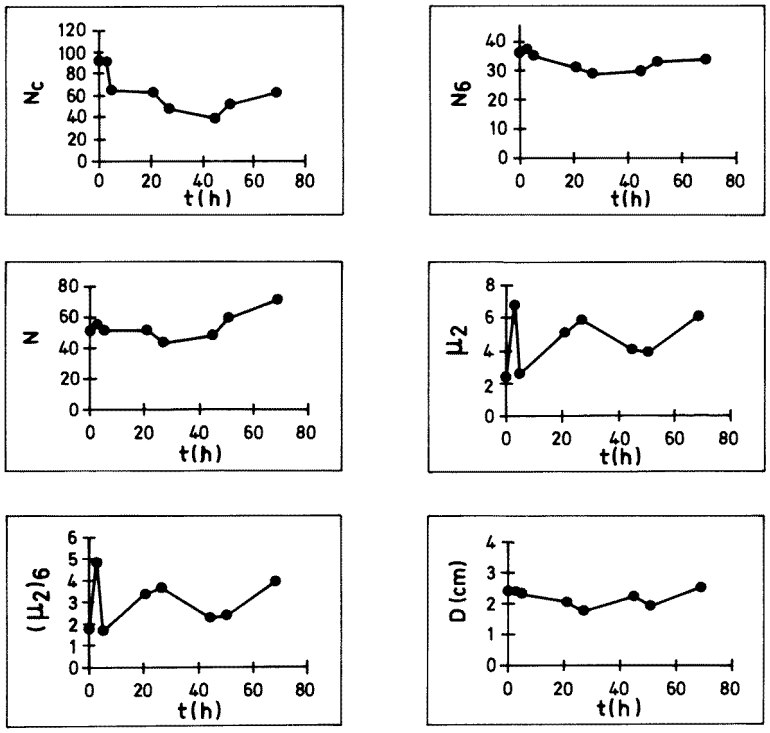

Figure 7. Evolution of various parameters of a type IIA defect cluster: N_c, N_6, N, μ_2, $(\mu_2)_6$ and diameter D.

Combining with von Neumann's equation yields, for $m \gg 6$,

$$k = \frac{3\pi}{32} a^2 \frac{\mathrm{d}m}{\mathrm{d}t}. \tag{7}$$

Typically $\mathrm{d}m/\mathrm{d}t \approx 0.1\ \mathrm{h}^{-1}$ for $a = 2$ mm (see figure 5). This gives

$$k = 0.12\ \mathrm{mm}^2\ \mathrm{h}^{-1}$$

which is one order of magnitude smaller than other literature values of k for aqueous/air foams at room temperature [9]. The relatively thick soap films in the froths used in the experiments are the probable reason for the smaller k.

It is also possible to obtain (from $A_m = \pi D^2/4$):

$$\frac{\mathrm{d}D}{\mathrm{d}t} = \frac{8}{\sqrt{3}\pi} \frac{k}{a}. \tag{8}$$

3.2. Type IIA clusters

The evolution of a type IIA cluster (cf figure 2) is shown in figure 6. The Burgers vector is $\bar{B} = 2\bar{b}$ (two pairs of extra half-rows). Plots of N_c, N_6, N, the second moments and D as a function of time are in figure 7.

The spreading of defects of this type is rather slow, with little change in N_6 over the duration of the experiment. Initially N_c is considerably larger than N, but decreases nearly

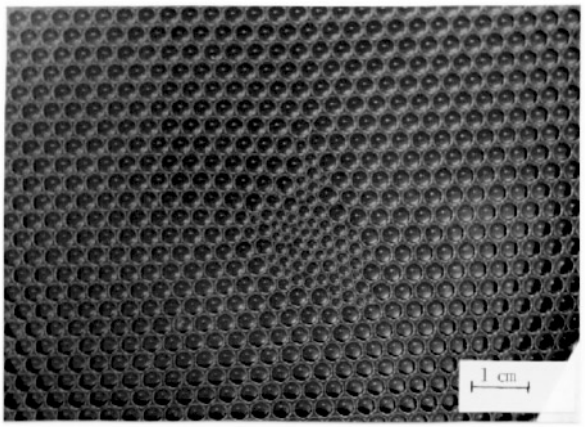

(a)

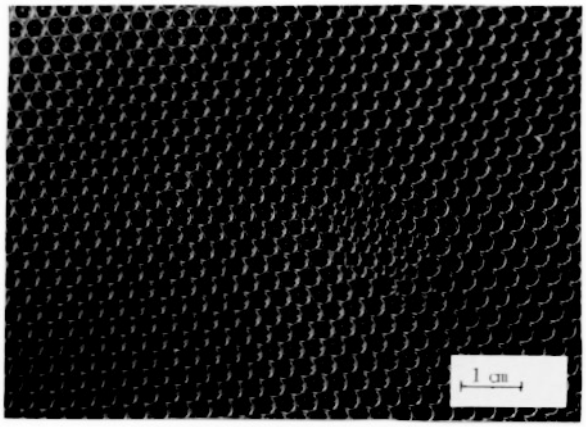

(b)

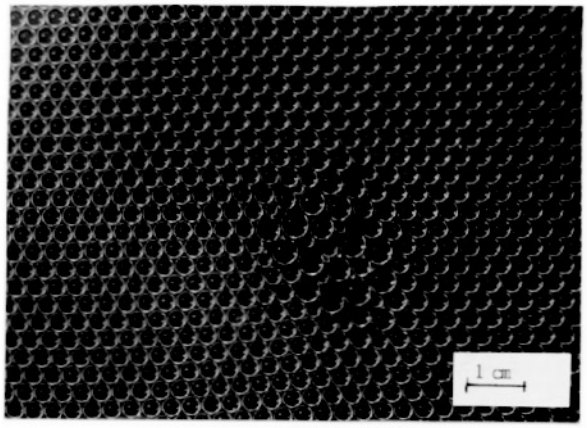

(c)

Figure 8. Evolution of a defect cluster of type IIB. (a) $t = 0$ h; (b) $t = 5$ h; (c) $t = 53$ h. The Burgers vector is $\bar{B} = \bar{b}$.

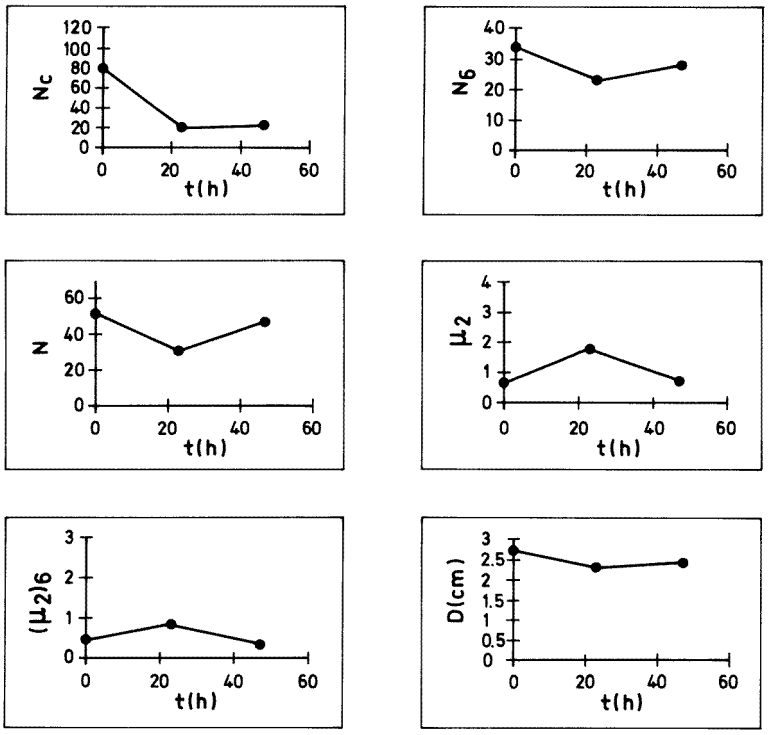

Figure 9. Evolution of various parameters of a type IIB defect cluster: N_c, N_6, N, μ_2, $(\mu_2)_6$ and diameter D.

to N after which both N_c and N tend to increase. The initial diameter of the clusters decreases slightly. The second moments tend to increase.

As the cluster grows, a gradient of cell size develops, with larger cells at the central region of the cluster. This gradient also occurs (and increases with time) in type I clusters, since the area of the large cell in these clusters increases with time while the adjacent defect cells have, on average, a constant area.

3.3. Type IIB clusters

A cluster of type IIB (cf figure 2) is shown in figure 8 at various times. The cluster evolves to resemble a type IIA defect, with a few cells growing to a relatively large area.

The evolution of N_c, N_6, N, the second moments and D, shown in figure 9, is broadly similar to that for type IIA clusters, with the same initial decrease in diameter.

3.4. Grain boundaries

An example of the evolution of a grain boundary defect is provided in figure 10 for a misorientation angle close to 30° (the misorientation angle is the smallest angle between close-packed rows in the two honeycombs).

The average number of sides of the defect varies between 5.70 and 6.07. The width increases with time (figure 11) but the data are not accurate enough to decide whether the variation is linear or not. The second moments vary irregulary with time.

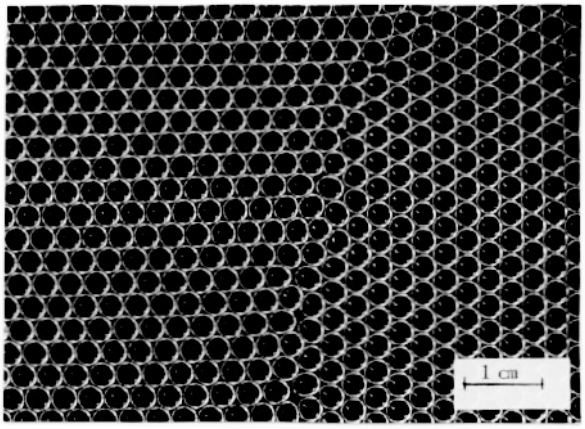

(a)

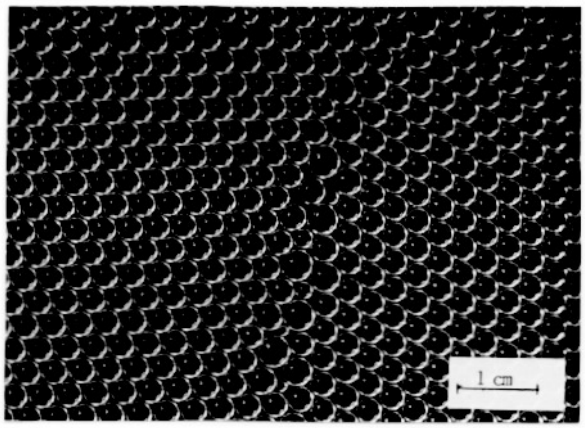

(b)

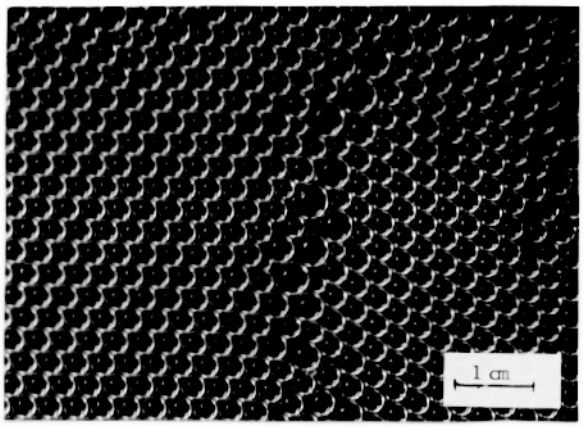

(c)

Figure 10. Evolution of grain boundary defect with misorientation $\theta \approx 30^\circ$. (a) $t = 0$ h; (b) $t = 69$ h; (c) $t = 142$ h.

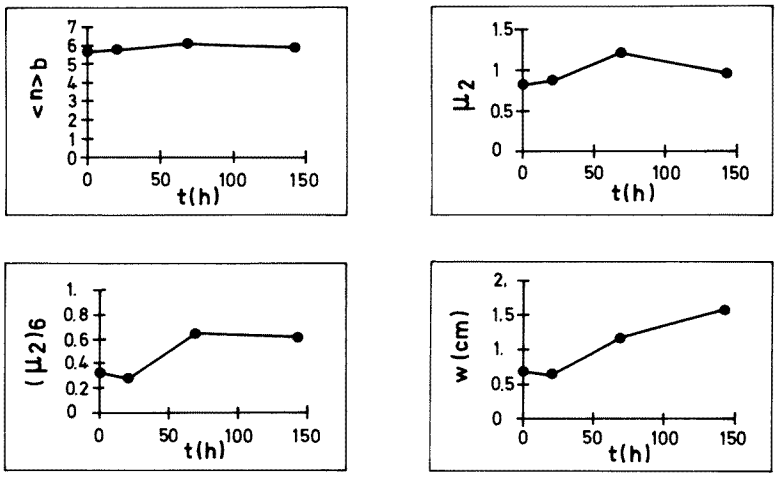

Figure 11. Evolution of various parameters of a grain boundary defect: $\langle n \rangle_b$, μ_2, $(\mu_2)_6$ and width w.

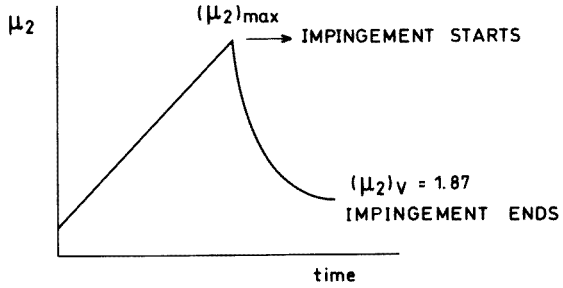

Figure 12. Predicted evolution of the global second moment of a system containing randomly distributed type I defect clusters with density $1/M$ (one defect per M honeycomb cells). The second moment reaches a maximum $(\mu_2)_{max} = 2\sqrt{3}M^{1/2}$ and then decreases to $(\mu_2)_V \approx 1.87$ when impingement of the growing clusters takes place.

As the grain boundary defect coarsens, a gradient of cell size develops in the direction of spreading, with the size decreasing as the distance to the original boundary increases.

4. Discussion

The experimental observations of defect spreading in hexagonal foams described in this paper are limited to relatively short periods and do not elucidate on the asymptotic behaviour at long times, which is the one usually studied in computer simulations. Nevertheless, the observations, in addition to providing the first experimental results on defect spreading, draw attention to new aspects that should be investigated in future computer simulations.

While the results for type I defect clusters generally agree with the predictions of computer simulations [2, 3], new aspects of the behaviour of type II (A and B) clusters have been found in the experiments. The development of a gradient of cell size, and the initial shrinking of type II clusters are perhaps the more relevant findings.

A defect cluster is separated from the surrounding hexagonal network by the 6-belt of 6-cells. The belt can be looked upon as a permeable and deformable wall around the cluster. If there is a net flow of the foam gas into the cluster, this wall will expand (incompressible gas) and the cluster will also expand. This may be called normal behaviour. In type I clusters, for which $N_c < N$, the average pressure inside the 6-belt is smaller than the outside pressure in the honeycomb cells and the clusters expand. The opposite happens in type II clusters for which $N_c > N$. Their small bubbles imply a larger pressure and gas flows out of the contracting cluster. The direction of flow eventually changes. The linear increase of radius with time in 'normal' clusters (that is $\mathrm{d}A_c/\mathrm{d}t \propto A_c^{1/2}$, where A_c is the area of the cluster) implies that ΔP, the average pressure difference between cluster and honeycomb gas, is a constant, independent of cluster size (and time).

The second moments μ_2 and $(\mu_2)_6$, in type I clusters and, at long times, also in type II clusters, increase while the cluster is invading the honeycomb. Suppose that there are various defect clusters of type I at time $t = 0$, with one cluster per M honeycomb cells ($M \gg 1$). Their rate of expansion $\mathrm{d}R/\mathrm{d}t$ is constant, the same for all clusters. Impingement of the growing clusters will occur at time τ, given approximately by $N_S^{-1/2}/(\mathrm{d}R/\mathrm{d}t)$ where N_S is the number of clusters per unit area, with $N_s = 1/(MA)$. Using (8) for $\mathrm{d}R/\mathrm{d}t$ (type I clusters) combined with (2) and (7), we obtain

$$\tau = (2\sqrt{3})^{1/2}\frac{M^{1/2}}{(\mathrm{d}m/\mathrm{d}t)}. \tag{9}$$

The second moment μ_2 of a type I cluster is approximately m (for $m \gg 6$). Therefore the second moment of the entire distribution of clusters at impingement time τ is

$$m(\tau) = \frac{\mathrm{d}m}{\mathrm{d}t}\tau \tag{10}$$

for $m(\tau) \gg m(0)$. This is the maximum second moment attained. Combining with (9) yields

$$(\mu_2)_{max} = m(\tau) = 2\sqrt{3}M^{1/2}. \tag{11}$$

Impingement of the growing clusters can be regarded as a Voronoi process of (simultaneous) nucleation and growth (isotropic, equal rate) of the original type I defect clusters. The resulting network is therefore a Voronoi network for which $(\mu_2)_V = 1.87$ [10]. We then expect a variation of the global μ_2 as schematically shown in figure 12, with an initial increase to $(\mu_2)_{max}$ followed by a quick decrease to $(\mu_2)_V$. This value is indeed close to, though slightly larger than, the one ($\mu_2 \approx 1.4$) that is usually accepted [5, 11, 12] as the second moment in the scaling regime of 2D foam coarsening. The Voronoi process assumes a constant growth rate, even after impingement starts. This may not be the case in an actual foam with type I defects since impingement of defects will occur at different times, and the growth characteristics of clusters may be altered upon impingement. This may explain the difference between the μ_2 value of the scaling regime and $(\mu_2)_V$. At any rate, it can be concluded that the steadily increasing second moment associated with the individual clusters is compatible with a scaling regime characterized by a low global second moment, which is reached after the growing clusters impinge on each other.

References

[1] Levitan B 1994 *Phys. Rev. Lett.* **72** 4057
[2] Ruskin H J and Feng Y 1995 *J. Phys.: Condens. Matter* **7** L553
[3] Jiang Y, Mombach J and Glazier J 1995 *Phys. Rev.* E **52** R3333

[4] Weaire D 1995 *Phys. Rev. Lett.* **74** 3710
[5] Herdtle T and Aref H 1992 *J. Fluid Mech.* **241** 233
[6] Fortes M A and Fátima Vaz M submitted
[7] el Kader A A and Earnshaw J C *Phil. Mag.* A at press
[8] von Neumann J 1952 *Metal Interfaces* (Cleveland, OH: American Society of Metals) p 108
[9] Glazier J A, Gross S P and Stavans J 1987 *Phys. Rev.* A **36** 306
[10] Crain I K 1978 *Comp. Geos* **4** 131
[11] Weaire D and Lei H 1990 *Phil. Mag. Lett.* **62** 47
[12] Stavans J and Glazier J A 1989 *Phys. Rev. Lett.* **62** 1318